



## Optimization of modified ABA<sup>2</sup> process using linearized ASM2 for saving aeration energy



Hyunook Kim<sup>a,\*</sup>, Honglae Lim<sup>b</sup>, Jinhyung Wie<sup>a</sup>, Ingyu Lee<sup>a</sup>, Mark F. Colosimo<sup>c</sup>

<sup>a</sup> Department of Energy and Environmental System Engineering, University of Seoul, 130-743 Seoul, Republic of Korea

<sup>b</sup> K-Water Corporation, 306-711 Daejeon, Republic of Korea

<sup>c</sup> International Joint Commission, U.S. Section, Washington, DC 20440, USA

### HIGHLIGHTS

- Simplified ASM2 model applied for predicting performance of ABA2 system.
- Simplified model-based MPC scheme designed to save aeration energy of ABA2 system.
- Pilot scale system controlled well to meet water quality limit set for effluent.
- MPC for ABA2 system saved about 19% aeration energy.

### ARTICLE INFO

#### Article history:

Received 3 January 2014  
Received in revised form 2 April 2014  
Accepted 18 April 2014  
Available online 26 April 2014

#### Keywords:

Activated sludge model  
Model predictive control  
Optimization  
Modified ABA<sup>2</sup>

### ABSTRACT

In the recent years, increasingly strict demands on the effluent quality of wastewater treatment plants (WWTPs) and concern for energy consumption have led to the growing interest in the development of an optimization and control scheme for treatment processes. In general, operation of WWTPs can be controlled either by real-time monitoring of major constituents or through model prediction. In this research, a simplified ASM2 model was applied to describe the dynamics of NH<sub>4</sub><sup>+</sup>, NO<sub>3</sub><sup>-</sup> and PO<sub>4</sub><sup>3-</sup> in a modified anaerobic, buffer, intermittently aerated, and oxic pilot-scale plant (treatment capacity = 50 m<sup>3</sup> d<sup>-1</sup>). Using this model, the system performance was optimized by adjusting aeration and non-aeration time to control effluent ammonia level to preset values and at the same time to minimize energy consumption for aeration. As a result of the operation, the system could achieve 89%, 73%, and 82% removal efficiencies for COD, TN, and TP, respectively. The average  $f_a$  (aeration cycle time/total cycle time) values were 0.46 for optimization as compared to 0.57 for normal operation. The standard errors between model predictions and measured effluent NH<sub>4</sub><sup>+</sup>-N were 0.1 mg L<sup>-1</sup> for the optimization scheme. With an application of optimizer, it can maintain good effluent water quality while achieving energy saving. For our pilot scale plant, it was calculated that annual electricity cost of about 600 USD could be saved if the plant would be continuously operated by the optimization scheme.

© 2014 Elsevier B.V. All rights reserved.

### 1. Introduction

For preventing eutrophication in lakes and streams, permit requirement on the effluent water quality of public wastewater treatment plants (WWTPs) has been much stricter, e.g., requirement changed from total Kjeldahl nitrogen (TKN) to total nitrogen (TN) concentration. Consequently, newly constructed WWTPs are designed as a biological nutrient removal (BNR) process capable of removing both nitrogen and phosphorus from wastewater. In addition, existing conventional WWTPs are also being upgraded

to BNR systems, especially temporal systems such as intermittently aerated activated sludge (IAAS) processes which, if properly controlled, can reduce energy consumption for aeration, and comply with permit requirement at the same time [1–3]. IAAS processes can oxidize ammonia to nitrate and uptake phosphate during aeration period, while it can reduce nitrate to nitrogen under anoxic conditions, and release phosphate under anaerobic conditions. In fact, a number of control strategies to optimize aeration duration have been proposed or performed for IAAS processes [4–9]. For example, Kim and Hao [10] compared a model based control scheme with on-line pH/ORP (oxidation reduction potential) sensor-based control for an IAAS system. They found that both control strategies could achieve significant energy

\* Corresponding author. Tel.: +82 2 6490 2871; fax: +82 2 2210 2917.

E-mail address: [h\\_kim@uos.ac.kr](mailto:h_kim@uos.ac.kr) (H. Kim).

savings. However, on-line pH/ORP sensor based control system does not require in-depth knowledge of WWTPs. The model based control scheme could flexibly adjust aeration time of the system according to the permit requirement [11–13].

Model predictive control (MPC) schemes have been widely used in industry [14]. In fact, a number of MPC strategies based on a mathematical model have been applied to control the biological process in WWTPs [8,15–18]. For the successful application of an MPC, the employed model should appropriately describe the behaviors of the target process. Numerous mathematical models have been introduced for describing the dynamics of BNR systems; for example, International Water Association's Activated Sludge Model No. 1 [19], ASM3 [5] for biological nitrogen removal and ASM2 [20], ASM2d [21,22], and UCTPHO+ [23] for biological nitrogen and phosphorus removal.

In this study, an MPC scheme based on a linearized model was applied to a modified anaerobic, buffer, intermittently aerated, and oxic (ABA<sup>2</sup>) pilot-scale plant for nitrogen and phosphorus removal. Influent and effluent characteristics of the pilot plant were continuously analyzed and fed into our MPC scheme for controlling effluent ammonia concentration with energy saving for aeration. The model used in our MPC scheme was previously developed by linearizing ASM2 [24,25].

## 2. Materials and methods

### 2.1. Description of pilot plant

The pilot-scale modified ABA<sup>2</sup> plant, located in Seonam WWTP in Seoul with a treatment capacity of 50 m<sup>3</sup> d<sup>-1</sup>, consists of an anaerobic reactor (hydraulic retention time (HRT): 1.0 h), a buffering tank (HRT: 0.5 h), an intermittently aerated reactor (HRT: 3.1 h), and another aeration basin (HRT: 0.9 h) (Fig. 1). Sludge recycle rate ( $Q_R$ ) was set half of the influent flow rate (0.5  $Q$ ). Internal recycle rate ( $Q_{IR}$ ) of mixed liquor suspended solids (MLSS) from the aeration basin to the buffering tank was set at the same flow rate of influent (i.e., 50 m<sup>3</sup> d<sup>-1</sup>). The DO concentration during aeration cycle times was maintained approximately at 2 mg L<sup>-1</sup> through a programmable logic controller. The aeration duration for the intermittently aerated reactor was determined by the MPC system. The mean cell residence time (MCRT) was set at 13 d to maintain the MLSS at 3500–3850 mg L<sup>-1</sup>. In order to evaluate the performance of the pilot plant, composite samples of influent and effluent were collected and analyzed following Standard Methods for COD, NH<sub>4</sub><sup>+</sup>, NO<sub>3</sub><sup>-</sup>, and TKN, total phosphorus (TP), PO<sub>4</sub><sup>3-</sup>, and suspended solids (SS) [26].

### 2.2. Development of simplified linear model

Since the main process (tank #3 in Fig. 1) of the pilot-scale modified ABA<sup>2</sup> system was intermittently aerated system for providing aerobic conditions for nitrification, phosphorus uptake, and organic oxidation with anoxic conditions for denitrification created after terminating aeration. In this study, NH<sub>4</sub><sup>+</sup>, NO<sub>3</sub><sup>-</sup>, and

PO<sub>4</sub><sup>3-</sup> dynamics of the intermittently aerated reactor were used for calibrating the model incorporated into the MPC scheme. The model for the MPC of the pilot system was formulated using the linearized ASM2 developed by [24,25]. Briefly, the hyperbolic terms in ASM2 [20] were linearized; 17 process equations, 17 state variables, and 46 stoichiometric and kinetic parameters in ASM2 were reduced to 10, 10, and 19, respectively, in the linearized model. Clearly, the linearized model requires less computational efforts for model calibration than the original ASM2.

Track studies were performed to characterize dynamic behaviors of NH<sub>4</sub><sup>+</sup>, NO<sub>3</sub><sup>-</sup>, and PO<sub>4</sub><sup>3-</sup> in the intermittently aerated reactor. The data from the track studies were then used to calibrate model parameters; the unknown parameters were hand-tuned to fit the model to the experimental data. Special care should be taken for  $J_4$ ,  $J_5$ , and  $J_{10}$ , since the model is quite sensitive to these parameters. Although the calibration was performed only once in this study, it can be done when mismatches between the model predicted NH<sub>4</sub><sup>+</sup> and the measured NH<sub>4</sub><sup>+</sup> become larger than 1.5 mg N L<sup>-1</sup>. Based on the calibrated model, optimization of the modified ABA<sup>2</sup> system was performed. More information of the model linearization can be found elsewhere [24].

### 2.3. Application of optimization scheme

The linearized model based optimization scheme is illustrated in Fig. 2. In the scheme, the control variables of the intermittently aerated reactor, i.e., one cycle time ( $t_c$ : aeration cycle time + non-aeration cycle time) and aeration ratio ( $f_a$ : aeration cycle time/ $t_c$ ) were adjusted to minimize the operation costs related to aeration as well as to satisfy the effluent NH<sub>4</sub><sup>+</sup> constraint. In order to prevent extended aeration or anoxic cycle, the maximum and minimum values were set for both  $t_c$  and  $f_a$ ; the maximum and minimum values set for  $t_c$  were 5.75 h and 1.5 h, respectively, and those set for  $f_a$  were 0.87 and 0.13. The predictions of the calibrated model were incorporated into the optimization scheme in which optimal  $t_c$

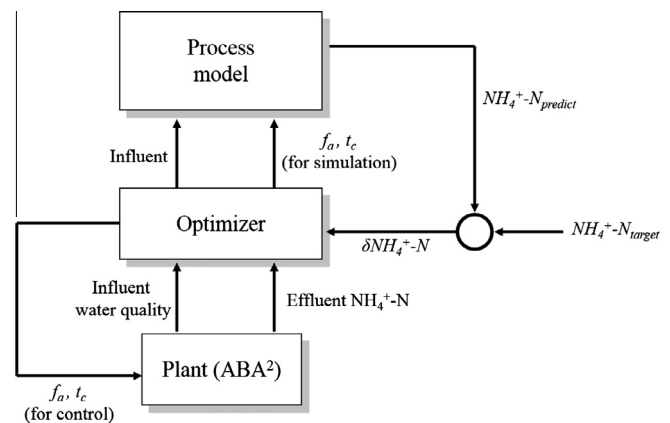


Fig. 2. Schematic diagram of optimization logic.

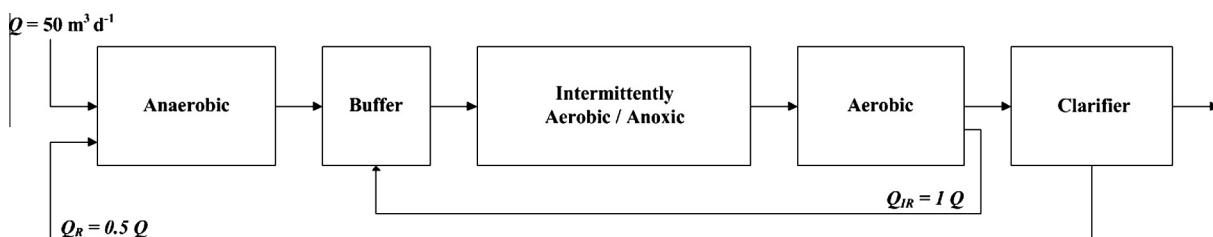


Fig. 1. Schematic diagram of ABA<sup>2</sup> plant.

and  $f_a$  values were determined. Influent and effluent water quality data measured from the plant were also fed into the optimization scheme, which used the developed model to predict the effluent water quality at different  $f_a$  and  $t_c$  (Fig. 2). The measured water quality data and model prediction were then compared to determine the optimal  $f_a$  for the system operation in the next day.

The mismatches between the model prediction and measured effluent values were corrected by a feedback loop algorithm (Fig. 2). Daily input data were total COD, soluble COD,  $\text{NH}_4^+$ ,  $\text{NO}_3^-$ , and  $\text{PO}_4^{3-}$  of influent wastewater and treated effluent. Since the control of the effluent  $\text{NH}_4^+$  concentration was the purpose of the current study, the  $f_a$  for the intermittently aerated reactor was adjusted to keep  $\text{NH}_4^+$ -N at the preset value of  $1.5 \text{ mg L}^{-1}$ . From the previous studies [21], it was found that if the aeration time required for nitrification is minimized, anoxic time for denitrification can be enlarged, resulting in reduction of effluent TN level. More information on the optimization procedure and error feedback scheme can be found in [25,27].

### 3. Results and discussions

#### 3.1. Overall performance

In Fig. 3, the performance of the pilot system for 90 d is presented. In the beginning, the system was operated with the preset  $f_a$  for the intermittently aerated reactor (Phase I);  $f_a$  was set at 0.57 (aeration time/ $t_c = 60 \text{ min}/105 \text{ min}$ ). Then the system was operated based on the proposed MPC for 50 d (Phase II).

In general, the modified ABA<sup>2</sup> system showed good performance. Influent and effluent characteristics along with operating conditions for the pilot plant are summarized in Table 1. Throughout Phases I–II, influent concentrations of COD, TKN, and TP fluctuated between 120–330, 17–39, and  $1.7\text{--}5.7 \text{ mg L}^{-1}$ , respectively. However, the system showed good COD, nitrogen, and phosphate removal efficiencies of 84–89%, 66–73%, and 72–82%, respectively at the overall HRT of the system of only 5.5 h.

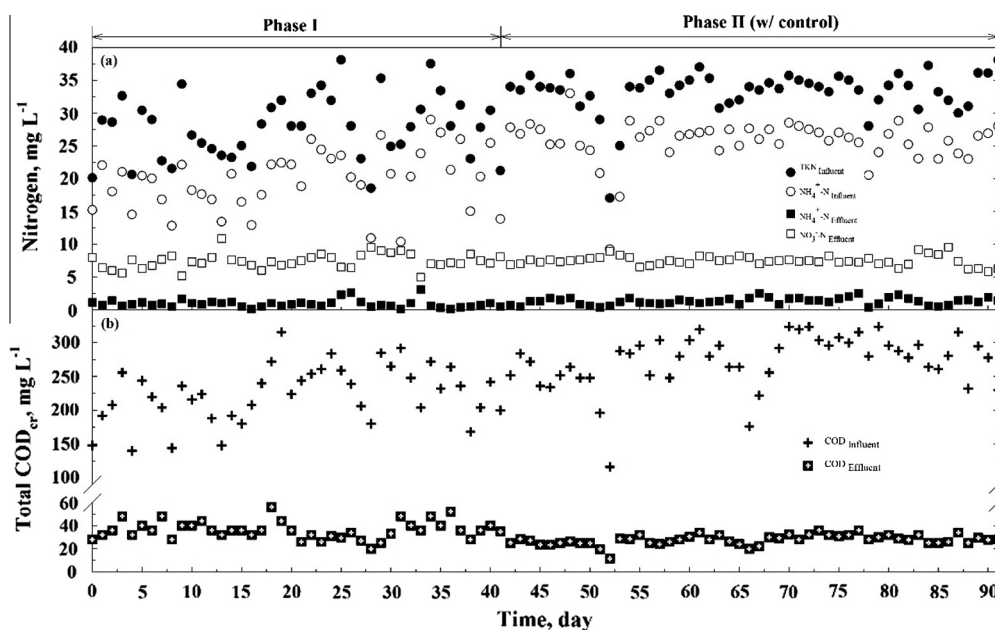


Fig. 3. Overall performance of ABA<sup>2</sup> system.

Table 1  
Performances of ABA<sup>2</sup> system.

Wastewater Characteristics	Phase I			Phase II (w/ control)		
	Influent $\text{mg L}^{-1}$	Effluent $\text{mg L}^{-1}$	Removal efficiency, %	Influent $\text{mg L}^{-1}$	Effluent $\text{mg L}^{-1}$	Removal efficiency, %
<i>Organic</i>						
Total COD	230 (140–320)	36	84	290 (120–330)	30 (12–40)	89
TN	28 (19–38)	9.4 (7.5–12)	66	37 (17–39)	9.9 (8.0–12)	73
TKN	28 (19–38)	1.5 (0.3–4.2)	95	37 (17–39)	2.4 (0.4–3.9)	94
$\text{NH}_4^+$ -N	20 (10–29)	0.9 (0.1–3.1)	95	26 (9.2–33)	1.4 (0.3–2.5)	95
$\text{NO}_3^-$ -N		7.4 (5.0–11)			7.5 (5.8–9.6)	
Phosphorus, TP	3.6 (1.7–5.7)	1.0 (0.1–1.5)	72	2.8 (1.9–3.8)	0.5 (0.2–0.9)	82
<i>Pilot plant conditions</i>						
Temp., °C	20.5–27.0			13.0–20.7		
MLSS, $\text{mg L}^{-1}$	3500 (3100–4000)			3900 (3500–4500)		
MCRT, d	13 (10–15)			13 (12–15)		
HRT, h	5.5			5.5		
Fraction ( $f_a$ )	0.57			0.46 (0.34–0.54)		
Total cyclic time ( $t_c$ ), min	105			126 <sup>a</sup>		
Air on/off time, h	1.0/0.75			1.1/1.0 <sup>a</sup>		

<sup>a</sup> Averaged value.

Fig. 4 shows the dynamics of  $\text{NH}_4^+$ ,  $\text{NO}_3^-$ , and  $\text{PO}_4^{3-}$  in the intermittently aerated reactor along with the system pH and ORP profiles. The significant points for indicating the end of nitrification/denitrification previously identified [18] were observed from the figure (e.g., ammonia valley (AV in Fig. 4c) on the pH profile, and nitrate knee (NK) on the ORP). In fact, the NK on the ORP profile which signifies complete denitrification during the air-off cycle was often not observed due to unavailability of easily biodegradable organics.

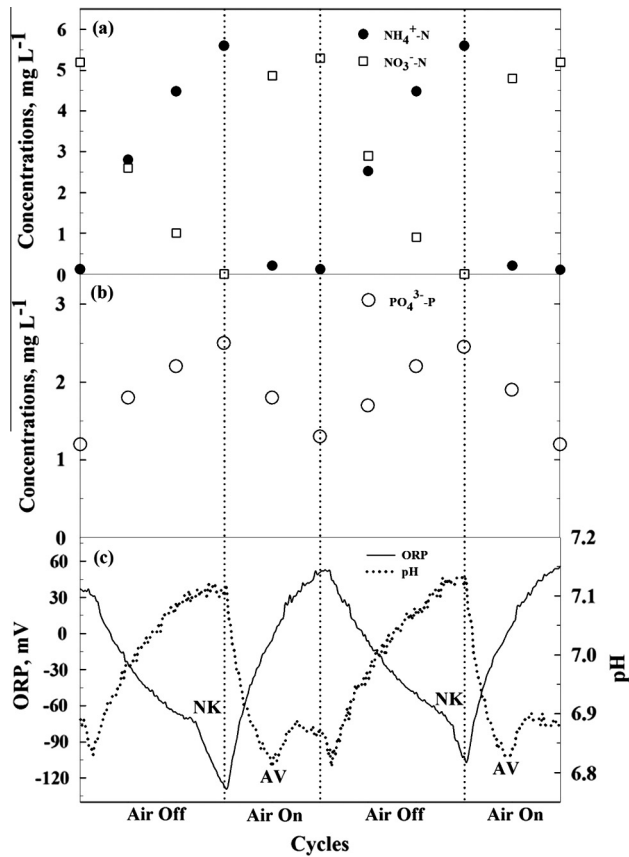


Fig. 4. Profile of nutrients and pH/ORP in intermittently aerated reactor.

### 3.2. Model calibration and evaluation

Before the MPC scheme was applied to the pilot system, the model used in this scheme was calibrated to describe dynamic behaviors of  $\text{NH}_4^+$ ,  $\text{NO}_3^-$ , and  $\text{PO}_4^{3-}$ . The simplified ASM2 was calibrated with a set of data from a track study on the intermittently aerated reactor. The calibrated values for corresponding stoichiometric and kinetic parameters are presented in Table 2, with the “ $J$ ” constants used in the linear model listed in Table 3. Each “ $J$ ” constant approximates non-linear Monod hyperbolic terms in the corresponding Monod equation of the original ASM2 model shown in [20]. For example, growth of heterotrophic microbial cells ( $\mu_H$ ) on fermentable organics ( $S_F$ ) is described with Eq. (1). As seen from the equation,  $\mu_H$  is influenced not only by  $S_F$  but also by fatty acids ( $S_A$ ), DO ( $S_{O_2}$ ),  $\text{NH}_4^+$  ( $S_{\text{NH}_4}$ ), phosphorus ( $S_{\text{PO}_4}$ ), and alkalinity ( $S_{\text{ALK}}$ ); influence of each variable on heterotrophic microbial cells ( $X_H$ ) is described in a saturation form with its associated half-saturation parameter. In the current model, the non-linear mathematical description in which influences from all the variables other than  $S_F$  was simplified (Eq. (2)) was approximated with a constant (in this case,  $J_2$ ).

$$\frac{dX_H}{dt} = \mu_H \cdot \frac{S_{O_2}}{K_{O_2} + S_{O_2}} \cdot \frac{S_F}{K_F + S_F} \cdot \frac{S_F}{S_F + S_A} \cdot \frac{S_{\text{NH}_4}}{K_{\text{NH}_4} + S_{\text{NH}_4}} \cdot \frac{S_{\text{PO}_4}}{K_P + S_{\text{PO}_4}} \cdot \frac{S_{\text{ALK}}}{K_{\text{ALK}} + S_{\text{ALK}}} \cdot X_H \quad (1)$$

$$\frac{dX_H}{dt} = \mu_H \cdot J_1 \cdot X_H \quad (2)$$

The parameters of linear model were manually fine-tuned using a trial-and-error procedure. Due to the less parameters of simplified model (19 parameters,  $J_1$ – $J_{10}$  constants) than full ASM2 (46 parameters), model calibration took less time and effort than that of the full model. The result of calibration is shown in Fig. 5. The simulation results from the simplified ASM2 (line) are plotted along with actual measured data (dot). In the calibration of the model, the stoichiometric coefficients were slightly adjusted and

Table 3  
“ $J$ ” constants used in this study.

	$J_1$	$J_2$	$J_3$	$J_4$	$J_5$	$J_6$	$J_7$	$J_8$	$J_9$	$J_{10}$
Phase II	4	10	10	10	5	3	0.1	200	150	350

Table 2  
Stoichiometric and kinetic parameters used in ABA<sup>2</sup> system.

Parameter (units)	ASM2 default	Current value	
$k_h$	Hydrolysis rate constant ( $\text{d}^{-1}$ )	3	2
$\eta_{\text{NO}_3}$	Anoxic hydrolysis reduction factor (-)	0.6	0.6
$\eta_{\text{Fe}}$	Anaerobic hydrolysis reduction factor (-)	0.4	0.4
$Y_H$	Heterotrophic yield ( $\text{g COD g}^{-1} \text{COD}$ )	0.63	0.63
$\mu_H$	Maximum growth rate on substrate ( $\text{d}^{-1}$ )	6	3
$q_{\text{Fe}}$	Maximum rate for fermentation ( $\text{g COD g}^{-1} \text{COD d}^{-1}$ )	3	1.5
$\eta_{\text{NO}_3}$	Reduction factor for denitrification (-)	0.8	0.8
$b_H$	Rate constant for lysis ( $\text{d}^{-1}$ )	0.4	0.65
$Y_{\text{PO}_4}$	PP requirement ( $S_{\text{PO}_4}$ release) for PHA storage ( $\text{g P g}^{-1} \text{COD}$ )	0.4	0.4
$Y_{\text{PHA}}$	PHA requirement for PP storage ( $\text{g COD g}^{-1} \text{P}$ )	0.2	0.3
$q_{\text{PHA}}$	Rate constant for storage of PHA ( $\text{g COD g}^{-1} \text{PAO d}^{-1}$ )	3	1.5
$q_{\text{PP}}$	Rate constant for storage of PP ( $\text{g PP g}^{-1} \text{PAO d}^{-1}$ )	1.5	2.5
$\mu_{\text{PAO}}$	Maximum growth rate ( $\text{d}^{-1}$ )	1	1
$b_{\text{PAO}}$	Rate constant for lysis of $X_{\text{PAO}}$ ( $\text{d}^{-1}$ )	0.2	0.1
$b_{\text{PP}}$	Rate constant for lysis of $X_{\text{PP}}$ ( $\text{d}^{-1}$ )	0.2	0.1
$b_{\text{PHA}}$	Rate constant for lysis of $X_{\text{PHA}}$ ( $\text{d}^{-1}$ )	0.2	0.1
$Y_{\text{AUT}}$	Yield coefficient (biomass/nitrate) ( $\text{g COD g}^{-1} \text{N}$ )	0.24	0.4
$\mu_{\text{AUT}}$	Maximum growth rate ( $\text{d}^{-1}$ )	1	0.3
$b_{\text{AUT}}$	Decay rate ( $\text{d}^{-1}$ )	0.1	0.01

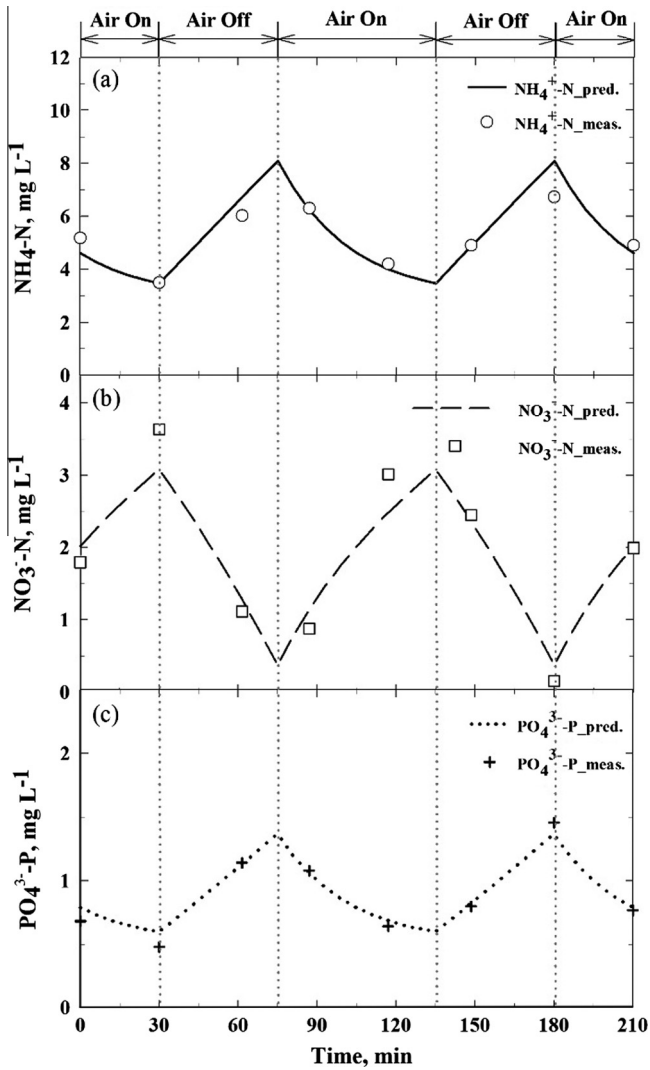


Fig. 5. Model calibration (air on/off time = 60/45 min).

applied to the kinetic parameters (see Table 2). Because the goal of model simplification is to develop a model that can be applied with less computational efforts, calibration was made mainly by adjusting linearized coefficients “J” terms. As shown in Fig. 5, the calibrated model describes reasonably well the biological reactions occurring in the intermittently aerobic reactor such as nitrification and phosphorus uptake during air-on periods and denitrification and phosphorus release during air-off periods (Phase II;  $R_{NH_4}^2$ : 0.91,  $R_{NO_3}^2$ : 0.86, and  $R_{PO_4}^2$ : 0.99) albeit with some mismatches observed for  $NH_4^+$  and  $NO_3^-$ . The simplified ASM2 was then incorporated into the optimization scheme to minimize aeration energy cost and to adjust effluent ammonium concentration to the preset values.

3.3. Optimization results

The calibrated model was used in the optimization scheme described in the previous section. The optimization results and overall performance of system in Phase II are presented in Fig. 6; data for Phase I were also included for comparison.

The constraint for the effluent  $NH_4^+$ -N concentration was set at  $1.5 \text{ mg L}^{-1}$ . Also, operating constraints for the minimum and maximum cycle times were set at 45 min and 4.5 h on the aeration and non-aeration cycle durations in order to avoid frequently turning aeration on/off and to ensure minimal durations for both aerobic and anoxic microbial reactions. Initially, the optimizer was run, assuming that a previous prediction was the same as the measurement with  $t_c$  and  $f_a$  set for 105 min and 0.57, respectively. The next day, the mismatch between the experimental measurement and the model prediction was incorporated into a corrective feedback loop to manipulate the  $t_c$  and  $f_a$  to make the effluent values match with the  $NH_4^+$  constraint. Through this procedure,  $t_c$  and  $f_a$  were determined as the variations of the  $NH_4^+$  effluent concentration, and the trend of effluent  $NH_4^+$ -N appeared as sinusoid around the  $NH_4^+$ -N<sub>max</sub> constraint (i.e.,  $1.5 \text{ mg L}^{-1}$ ). However, comparatively large mismatches between effluent data and predictions were often observed. It was due to the fact that the mismatches were caused by temperature variations and rainy events which were not incorporated into the optimization scheme (Phase II; day 35, 42, and 68 in Fig. 6). In those cases, the model was prone to underestimate or overestimate effluent  $NH_4^+$  level. Nonetheless, through

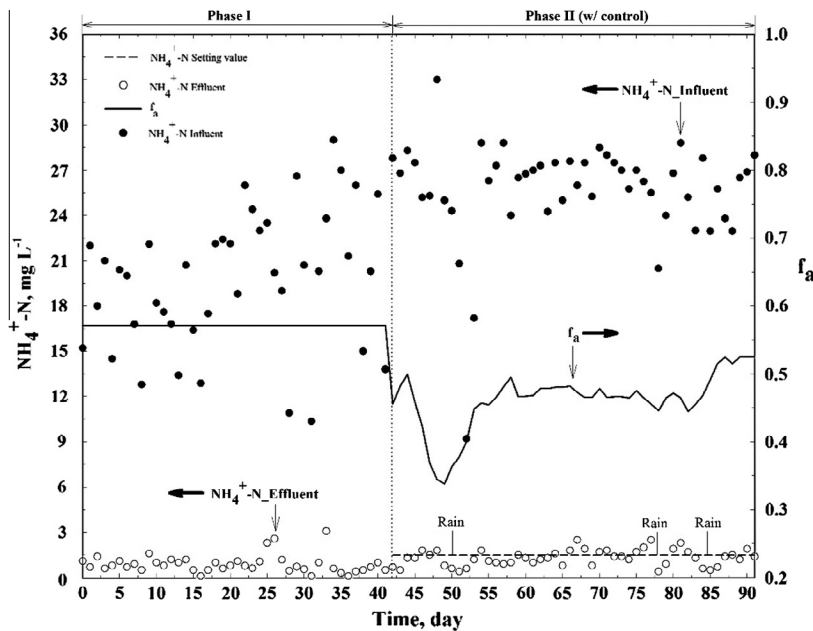


Fig. 6. Summary of optimization results.

the feedback control, the tendency of the  $\text{NH}_4^+$  profile around the set point is demonstrated despite of mismatched gap. It is expected that the width of this mismatch will be reduced when the simplified model takes account of adding the calibration scheme about temperature gradient.

Another control problem is due to raining event. For example, the effluent  $\text{NH}_4^+\text{-N}$  was found to be  $0.4 \text{ mg L}^{-1}$  on day 69 due to rainy weather. Then,  $f_a$  was changed from 0.40 to 0.38; the  $f_a$  was further lowered three consecutive days to 0.34 (day 71) due to low influent of  $\text{NH}_4^+$  concentrations. The trend is attributed to the fact that  $\sigma\text{NH}_4^+\text{-N}$  (mismatch between observed and preset values) in the optimization routine relies both on the mismatches occurring in the past and the one in the present, i.e., the previous conditions were reflected in the current data based on the accumulated  $\sigma\text{NH}_4^+\text{-N}$ . Therefore,  $f_a$  values should not be changed rapidly, and then the gap between predictions and experimental data caused by sudden unforeseen events could be minimized.

The average effluent ammonia concentration during the applied optimization scheme was  $1.4 \text{ mg L}^{-1}$  ranging from  $0.3$  to  $2.5 \text{ mg L}^{-1}$  with 73% TN removal efficiency. During the operation, the optimizer increased the  $f_a$  value up to 0.52 and lowered down to 0.34, according to influent characteristics. As stated above, by minimizing the aeration cycle duration for nitrification, the anoxic duration was enlarged resulting in the high TN removal even with the relatively short HRT of 5.5 h.

#### 4. Conclusions

In this study, it has been demonstrated that if an MPC system is used, the modified ABA<sup>2</sup> system could show good performance in removing COD, TN and TP as well as saving aeration energy. The ASM2 was simplified to a linear model by replacing Monod hyperbolic terms with first-order rate constants (i.e.  $J_s$ ), and the simplified model was applied to predict the nutrient dynamics of the modified ABA<sup>2</sup> process. The model could capture the characteristic dynamics of the system well according to the corresponding aerobic/anoxic cycle changes in the intermittently aerated reactor. The prediction of the model was incorporated in an MPC system to optimize the aeration cycle time. After the calibration was performed, the pilot plant was operated for 40 d using the MPC system, in which effluent  $\text{NH}_4^+$  was set at  $1.5 \text{ mg N L}^{-1}$ . Due to the aeration optimization based on the MPC, the average effluent ammonia concentration was  $1.4 \text{ mg N L}^{-1}$  even in the spring season. The standard error between model predictions of effluent  $\text{NH}_4^+\text{-N}$  with measurements was  $0.1 \text{ mg L}^{-1}$ . In addition,  $f_a$  values were minimized at average of 0.46. Comparing data from Phase I (fixed  $f_a$ ) and Phase II (controlled  $f_a$ ), the control system could achieve high TN removal efficiency with significant aeration energy saving. Comparing with the plant operation without the optimization scheme, the optimization-based operation was found to save about 600 USD annually.

In short, an optimization scheme was accomplished successfully in spite of seasonal variations of influent characteristics and temperature to minimize aeration cost and maintain acceptable effluent concentrations for ammonia and other water quality parameters.

#### Acknowledgment

This work was supported by the R&D program of MOTIE/KEIT (R&D Program No.: 10037331, Development of Core Water Treatment Technologies based on Intelligent BT-NT-IT Fusion Platform).

#### References

- [1] A. Dey, D.D. Truax, B.S. Magbanua, Optimization of operating parameters of intermittent aeration-type activated sludge process for nitrogen removal: a simulation-based approach, *Water Environ. Res.* 83 (2011) 636–642.
- [2] G. Dotro, B. Jefferson, M. Jones, P. Vale, E. Cartmell, T. Stephenson, A review of the impact and potential of intermittent aeration on continuous flow nitrifying activated sludge, *Environ. Technol.* 32 (2011) 1685–1697.
- [3] J. Huang, O.J. Hao, Alternating aerobic–anoxic process for nitrogen removal: dynamic modeling, *Water Environ. Res.* 68 (1996) 94–104.
- [4] D. Gao, X. Yuan, H. Liang, W.M. Wu, Comparison of biological removal via nitrite with real-time control using aerobic granular sludge and flocculent activated sludge, *Appl. Microbiol. Biotechnol.* 89 (2011) 1645–1652.
- [5] W. Gujer, M. Henze, T. Mino, M.V. Loosdrecht, Activated sludge model no. 3, *Water Sci. Technol.* 39 (1) (1999) 183–193.
- [6] O. Hanhan, G. Insel, N.O. Yagci, N. Artan, D. Orhon, Mechanism and design of intermittent aeration activated sludge process for nitrogen removal, *J. Environ. Sci. Health A* 46 (1) (2011) 9–16.
- [7] R. Marquez, M. Blandria-Carvajal, C. Gómez-Quintero, M. Rios-Bolivar, Average modeling of an alternating aerated activated sludge process for nitrogen removal, in: *World Congress*, vol. 18, 2011, pp. 14195–14200.
- [8] M. O'Brien, J. Mack, B. Lennox, D. Lovett, A. Wall, Model predictive control of an activated sludge process: a case study, *Control Eng. Pract.* 19 (2011) 54–61.
- [9] G. Olsson, Automation development in water and wastewater systems, *Environ. Eng. Res.* 12 (2007) 197–200.
- [10] H. Kim, O.J. Hao, pH and oxidation–reduction potential control strategy for optimization of nitrogen removal in an alternating aerobic–anoxic system, *Water Environ. Res.* 73 (2001) 95–102.
- [11] L. Amanda, B. Carlsson, Optimal aeration control in a nitrifying activated sludge process, *Water Res.* 46 (2012) 2101–2110.
- [12] A.C. de Araújo, S. Gallani, M. Mulas, G. Olsson, Systematic approach to the design of operation and control policies in activated sludge systems, *Ind. Eng. Chem. Res.* 50 (2011) 8542–8557.
- [13] T.Y. Huang, N. Li, Y. Huang, Modeling of nitrogen removal and control strategy in continuous-flow-intermittent-aeration process, *Afr. J. Biotechnol.* 11 (2012) 10626–10631.
- [14] J. Richalet, A. Rault, J.L. Testud, J. Papon, Model predictive heuristic control: applications to industrial processes, *Automatica* 14 (1978) 413–428.
- [15] M.N. Bourmazou, K. Hooshier, H. Arellano-Garcia, G. Wozny, G. Lyberatos, Model based optimization of the intermittent aeration profile for SBRs under partial nitrification, *Water Res.* 47 (2013) 3399–3410.
- [16] F.J. Fernandez, M.C. Castro, M.A. Rodrigo, P. Canizares, Reduction of aeration costs by tuning a multi-set point on/off controller: a case study, *Control Eng. Pract.* 19 (2011) 1231–1237.
- [17] D. Vreko, N. Hvala, M. Straar, The application of model predictive control of ammonia nitrogen in an activated sludge process, *Water Sci. Technol.* 64 (2011) 1115–1121.
- [18] G. Zhu, Y. Peng, B. Ma, Y. Wang, C. Yin, Optimization of anoxic/oxic step feeding activated sludge process with fuzzy control model for improving nitrogen removal, *Chem. Eng. J.* 151 (2009) 195–201.
- [19] M. Henze, C.P.L. Grady Jr., W. Gujer, G.V.R. Marais, T. Matsuo, Activated Sludge Model No. 1: IAWPRC Scientific and Technical Report No. 1, IAWPRC, London, 1987.
- [20] W. Gujer, M. Henze, T. Mino, T. Matsuo, M.C. Wentzel, G.V.R. Marais, The activated sludge model no. 2: biological phosphorus removal, *Water Sci. Technol.* 31 (2) (1995) 1–12.
- [21] P.S. Barker, P.L. Dold, General model for biological nutrient removal activated-sludge systems: model presentation, *Water Environ. Res.* 69 (1997) 969–984.
- [22] M. Henze, W. Gujer, T. Mino, T. Matsuo, M.C. Wentzel, G.V.R. Marais, M.V. Loosdrecht, Activated sludge model no. 2d., ASM2d, *Water Sci. Technol.* 39 (1) (1999) 165–182.
- [23] Z.R. Hu, M.C. Wentzel, G.A. Ekama, A general kinetic model for biological nutrient removal activated sludge systems: model development, *Biotechnol. Bioeng.* 98 (2007) 1242–1258.
- [24] H. Kim, O.J. Hao, T.J. McAvoy, SBR system for phosphorus removal: ASM2 and simplified linear model, *J. Environ. Eng. – ASCE* 127 (2001) 98–104.
- [25] H. Kim, O.J. Hao, T.J. McAvoy, SBR system for phosphorus removal: linear model based optimization, *J. Environ. Eng. – ASCE* 127 (2001) 105–111.
- [26] American Public Health Association (APHA), American Water Works Association (AWWA), Water Environment Federation (WEF), Standard Methods for the Examination of Water and Wastewater, 22 ed., 2012.
- [27] H. Kim, T.J. McAvoy, J.S. Anderson, O.J. Hao, Control of an alternating aerobic–anoxic activated sludge system—Part 2: Optimization using a linearized model, *Control Eng. Pract.* 8 (2000) 279–289.